Documentations for IBM Open Science Prize Submission

Yufeng Bright Ye[1] and Lingbang Zhu[2]

[1]Department of Electrical Engineering and Computer Science, MIT, Cambridge, MA 02139
[2]Department of Chemistry and Chemical Biology, Harvard, Cambridge, MA, 02138

April 2022

Abstract

We perform quantum simulation of a homogeneous (XXX) Heisenberg model of three spins on IBM Jakarta. We implement several approaches to improve the final state fidelity: 1. Trotterization optimization via symmetry protection on re-ordered terms, 2. Pulse optimization using short RZX gates instead of the native CX gates, 3. Error mitigation including standard measurement error mitigation and zero-noise (Richardson) extrapolation with pulse stretching. As shown in Table 1, with each additional optimization, we increase our final state fidelity from 3.8% (given by the sample code) to eventually $86.9 \pm 0.9\%$ on IBM Jakarta.

	Default	Re-ordered & symmetry	Pulse optimized RZX	Meas. error mit.	Zero-noise extrap.
F_{avg}	$3.8 \pm 0.1\%$	46.6 %	70.3 ± 0.4 %	77.0 ± 0.4 %	86.9 ± 0.9 %

Table 1: Experimental average final state fidelity using various techniques. Result in every column includes optimizations of all columns to the left (except default).

1 Trotterization optimization

The objective is to simulate the Heisenberg XXX model for 3 spins (labelled 0,1,2):

$$H_{\text{Heis3}} = \sigma_x^{(0)}\sigma_x^{(1)} + \sigma_x^{(1)}\sigma_x^{(2)} + \sigma_y^{(0)}\sigma_y^{(1)} + \sigma_y^{(1)}\sigma_y^{(2)} + \sigma_z^{(0)}\sigma_z^{(1)} + \sigma_z^{(1)}\sigma_z^{(2)}.$$

using Trotterization.

In this section, we explore different Trotterization strategies (see Fig. 1) to optimize for the highest theoretical (noiseless) fidelity with the fewest Trotter steps (see Fig. 2).

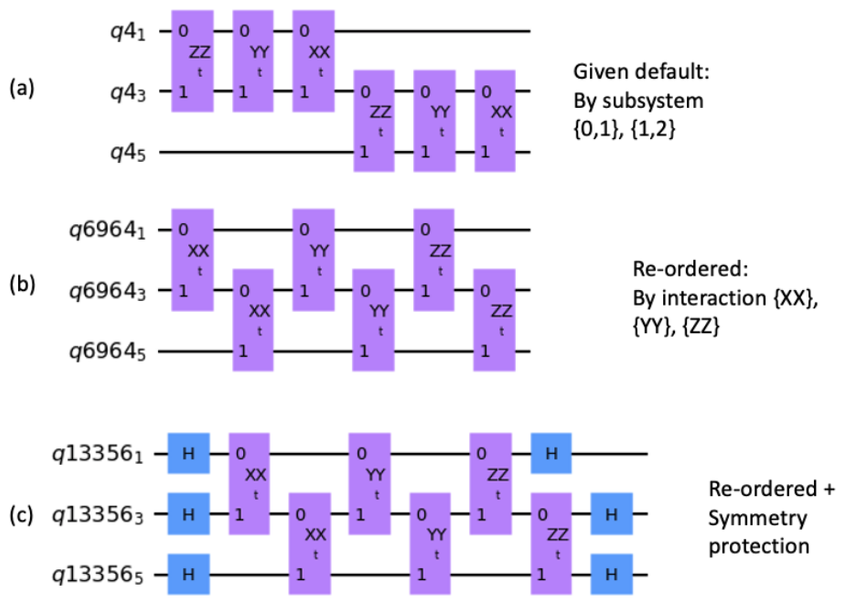

Figure 1: Different Trotterizations: gates in one Trotter step. For 1c (with symmetry protection), the Trotter step for an odd number step is shown (even number step is same as 1b).

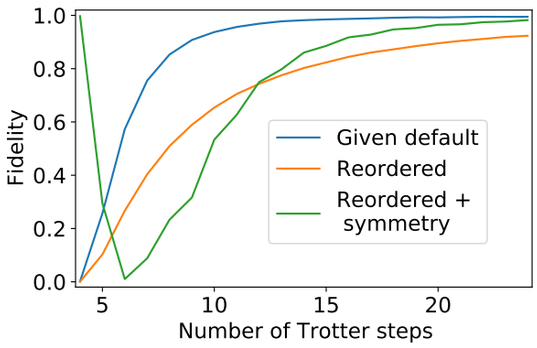

Figure 2: Fidelity versus number of Trotter steps for three different Trotterization strategies, results are from noiseless simulator and cover every Trotter step $\in [4, 25)$.

1.1 Given default (by subsystem)

In the default code provided, the Trotterization split the interaction into two subsystems (between spin 0,1 and spin 1,2):

$$U_{\text{Heis3}}(t) = \exp\left[-it\left(H^{(0,1)}_{\text{Heis2}} + H^{(1,2)}_{\text{Heis2}}\right)\right] \tag{1}$$

$$\approx \left[\exp\left(\frac{-it}{n}H^{(0,1)}_{\text{Heis2}}\right)\exp\left(\frac{-it}{n}H^{(1,2)}_{\text{Heis2}}\right)\right]^n. \tag{2}$$

where $H^{(i,j)}_{\text{Heis2}} = \sigma^{(i)}_x\sigma^{(j)}_x + \sigma^{(i)}_y\sigma^{(j)}_y + \sigma^{(i)}_z\sigma^{(j)}_z$ is the interaction within each two-spin subsystem. See Fig. 1a for the gate sequence with this default Trotterization.

1.2 Re-ordered (by interaction)

For this and the following subsection, we follow the recent work of Tran et al. 2021 [1]. They grouped Hamiltonian terms not by spins subsystems but by interactions instead (see ref. [1]'s Eqn. [34-35]). As shown below:

$$U_{\text{Heis3}}(t) = \exp\left[-it(H_X + H_Y + H_Z)\right] \tag{3}$$

$$\approx \left[\exp\left(\frac{-it}{n}H_X\right)\exp\left(\frac{-it}{n}H_Y\right)\exp\left(\frac{-it}{n}H_Z\right)\right]^n \tag{4}$$

where

$$H_X = \sigma^{(0)}_x\sigma^{(1)}_x + \sigma^{(1)}_x\sigma^{(2)}_x,$$
$$H_Y = \sigma^{(0)}_y\sigma^{(1)}_y + \sigma^{(1)}_y\sigma^{(2)}_y,$$
$$H_Z = \sigma^{(0)}_z\sigma^{(1)}_z + \sigma^{(1)}_z\sigma^{(2)}_z.$$

each X, Y, Z interaction terms are grouped together for all spins. See Fig. 1b for the gate sequence with this re-ordered Trotterization.

As shown in Fig. 2, the fidelity of this re-ordered Trotterization sequence is lower at all Trotter steps than the given default. But as we'll see in the subsection below, this Trotterization sequence allows for symmetry protection which will boost performance significantly.

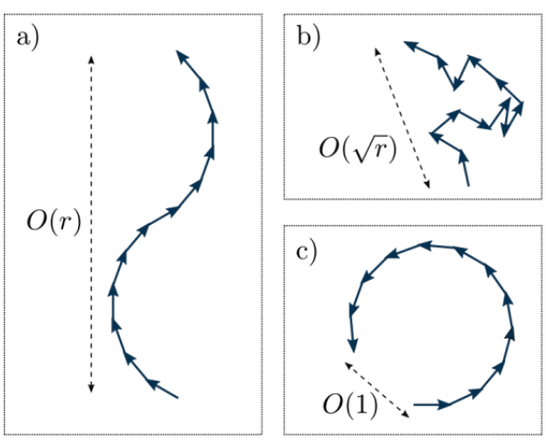

Figure 3: Figure from Tran et al. [1] explaining the intuition behind symmetry protection: Errors from each Trotter step (small vectors) are cancelled by making symmetry transformations (b,c) between steps. Compared to case without symmetry transforms (a), the total cumulative error (dashed line) with symmetry protection is smaller (b) or in some cases close to zero (c).

1.3 Re-ordered + symmetry protection

We first summarize the intuition behind Tran et al. [1]'s symmetry protection scheme. As shown in Fig. 3 taken from [1]: Errors from each Trotter step (small vectors) are cancelled by making symmetry transformations (subpanel b,c) between steps. Compared to case without symmetry transforms (subpanel a), the total cumulative error (dashed line) with symmetry protection is smaller (subpanel b) or in some cases close to zero (subpanel c).

For our Heisenberg XXX Hamiltonian, which is invariant under $SU(2)$, the symmetry transformations are the unitaries that simultaneously rotate all spins by the same angle in their Bloch sphere. In fact, it was derived in Eqn. (37-39) of [1] that the optimal symmetry protecting unitary (for the re-ordered Trotterization by interaction) is the Hadamard gate. Therefore, as shown in Fig. 1c, we insert Hadamard gates between every other Trotter steps of Fig. 1b (following Eqn. (39) of ref. [1]).

As shown in Fig. 2, this symmetry protection significantly improves fidelity (over just the re-ordered case) at all Trotter steps except 6-10. In particular, at Trotter step = 4 (the minimal allowed in this competition), the re-ordered Trotterization with symmetry protection can reach near perfect fidelity. Hereafter, we will only use 4 Trotter steps of re-ordered Trotterization with symmetry since it achieves such high theoretical fidelity with the minimal number of Trotter steps. Using the minimal 4 Trotter steps minimizes circuit depth and should translate to high fidelity on experimental device.

Although re-ordered Trotterization with symmetry seems slightly worse than the given default Trotterization at large Trotter steps, this comparison is largely meaningless. The proper comparison should be between given default and given default with symmetry protection to see the effect of symmetry protection, however Tran et al. [1] hasn't calculated what the right symmetry protection unitaries are for the given default Trotterization, so we are going with re-ordered Trotterization to be consistent with their results.

2 Pulse optimization

2.1 Native CX gates

Using re-ordered terms and symmetry protected Trotterization with 4 Trotter steps, we obtained 46.6% fidelity for the final state (Table 1); this is by using the default gates with native CX for all XX, YY and ZZ gates (Fig. 4a).

2.2 Pulse efficient RZX gates

In the default circuit given, every XX, YY and ZZ gate is decomposed into 2 CX gates and multiple single-qubit gates (Fig. 4a). Since the native CX gates take relatively long time, we can shorten the pulse length for each trotter step with a more time-efficient construction of XX, YY and ZZ gates.

It has been demonstrated [1, 2, 3] that one XX, YY or ZZ gate could be decomposed into one RZX gate (two with echo) with a few single qubit gates as shown in Fig. 4b.

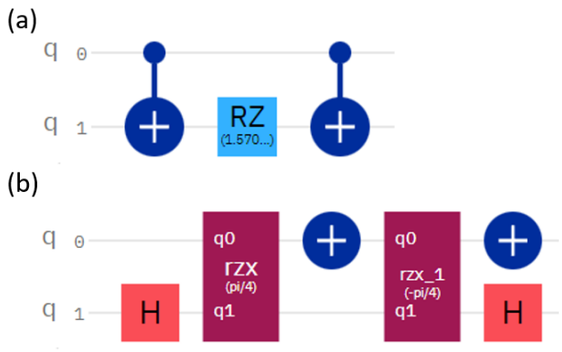

Figure 4: (a) The default way of creating ZZ gate from native CX gates, (b) the pulse-efficient way to create ZZ gate using Hadamard and echoed RZX gates

From Fig. 5, after replacing the original native CX gates with a series of pulse efficient RZX gates from ref. [3], the time consumption for one Trotter step decreased from 18.7k cycles to 9.1k cycles, which represents a total time reduction of about 50%. However, the total pulse schedule (not one but four Trotter steps) time is reduced from 100k to 60k cycles (see Appendix Fig. 9). This reduction is not 50% because the readout sequence takes some time.

The shortening of the pulse schedule leads to a significant increase to the fidelity of our final state, from about 47% to 70% (Table 1). This improvement suggests that shortening the pulse schedule time could protect the system from T_1 and T_2 errors.

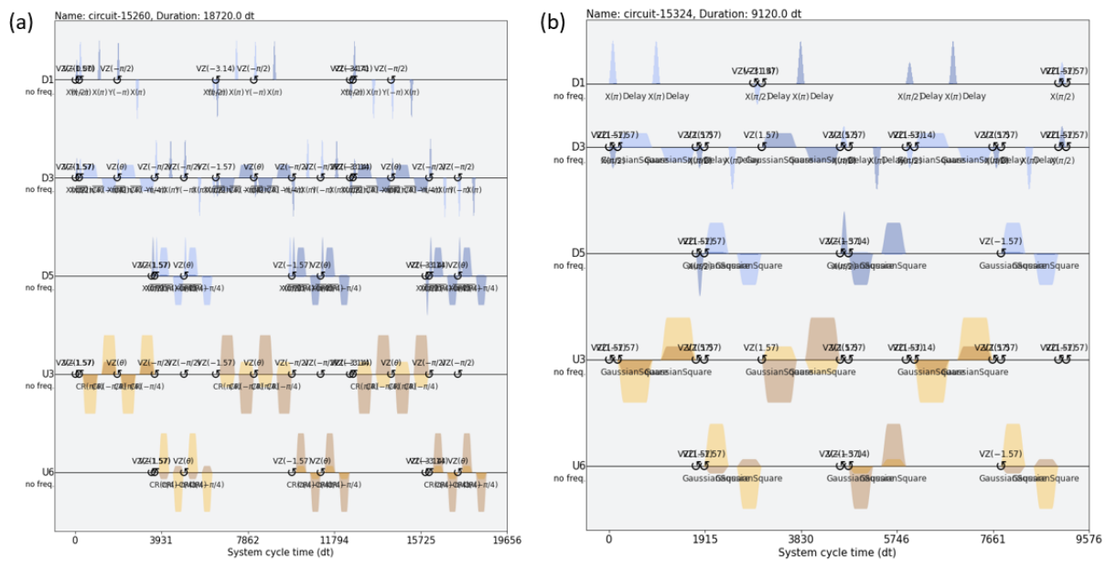

Figure 5: (a) The pulse schedule for 1 Trotter step using the native CX gates. (b) Optimized pulse schedule for 1 Trotter step using echoed RZX gates.

3 Error mitigation

In addition to optimized Trotterization gate sequence and optimized pulse-efficient RZX gates from the two previous sections, we further post-process results with error mitigation techniques to improve fidelity.

3.1 Measurement error mitigation

First, we apply standard measurement error mitigation [4] by accounting for the measurement assignment errors for the three qubits. We perform a measurement to map out the calibration matrix that shows the probability of measuring all basis states for each state we prepare them in. From Fig. 6, we notice that the main source of measurement error is single qubit flips.

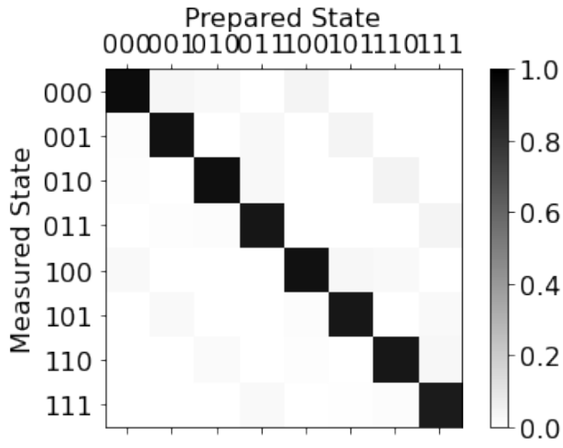

Figure 6: The calibration matrix for measurement errors

By applying 'complete' measurement error mitigation [4] with this calibration matrix to experimental result counts, we obtain a post-mitigation average fidelity of 77.0 ± 0.4 %, about 7% higher compared to our previous un-mitigated result (Table 1).

3.2 Zero-Noise (Richardson) Extrapolation

We perform Richardson extrapolation [5] by stretching and squeezing our pulses for the RZX gates. We make sure that the Gaussian-square areas for the drive pulses are preserved under such transformations.

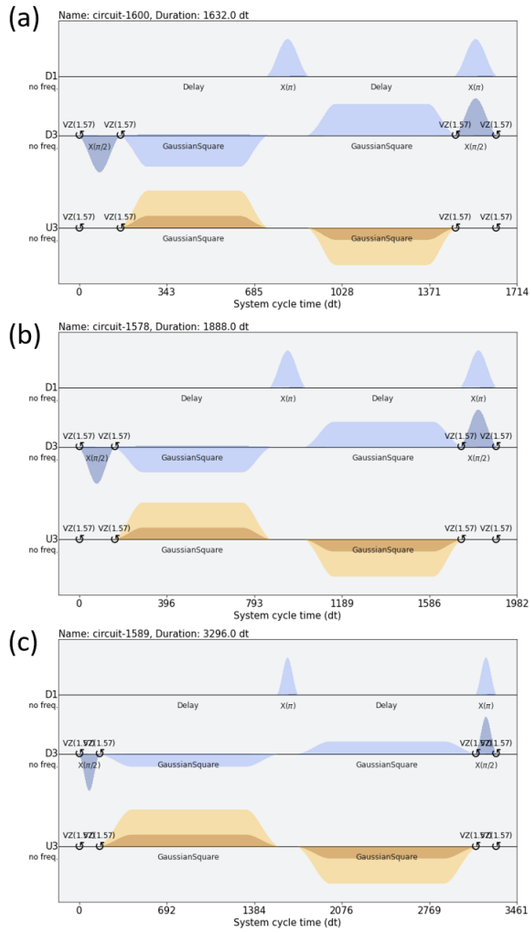

Figure 7: One ZZ gate pulse schedule (a): Pulse temporal stretch factor equals to 0.8 (b): Pulse temporal stretch factor equals to 1.0 (c): Pulse temporal stretch factor equals to 2.0

We run circuits with different stretch factors ranging from 0.82 to 2.5 and fit every basis state expected value (by fitting their measurement counts) versus stretch factor using a linear model [5]. To be more specific, we perform a separate linear fit for each basis result count from the 8 repetitions of the 27 state tomography circuits each with 2^3 basis states measurements ('000','001', etc) Then we extrapolate the fitted counts (note that we don't fit the fidelity vs stretch factor as it is not allowed) to the smallest possible pulse stretch factor. This extrapolation is limited because the fit at near-zero stretch factor has high uncertainty and can return negative counts which is both unphysical and causes errors in subsequent state tomography fitting. After extrapolation for all 2^3 basis state counts from a particular experimental run is complete, we re-normalize the extrapolated counts so they again sum to the original shot number 8192.

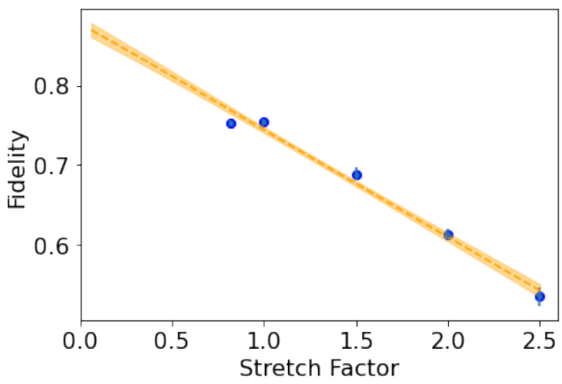

Figure 8: Richardson extrapolation (applied to state before fidelity calculation) improves fidelity for smaller extrapolated stretch factors (points = experimental stretched pulse results used for fit, dashed = fit extrapolation results, shaded = ± 1 standard deviation of fit extrapolation). Measurement error mitigation applied.

The result of the Richardson extrapolation (with measurement error mitigation included) is shown in Fig. 8. It is clear that the post-processed state with extrapolated counts has significantly higher state fidelity (87% vs 75%).

We also emphasize that the noise level of the Jakarta machine has significant day-to-day fluctuations. As an extreme example, when we performed our Richardson extrapolation measurements in early April 2022, the fidelity we obtained are sometimes as low as 74% (after extrapolation). But in all cases, significant fidelity improvements are obtained with zero-noise extrapolation compared to without.

4 Appendix

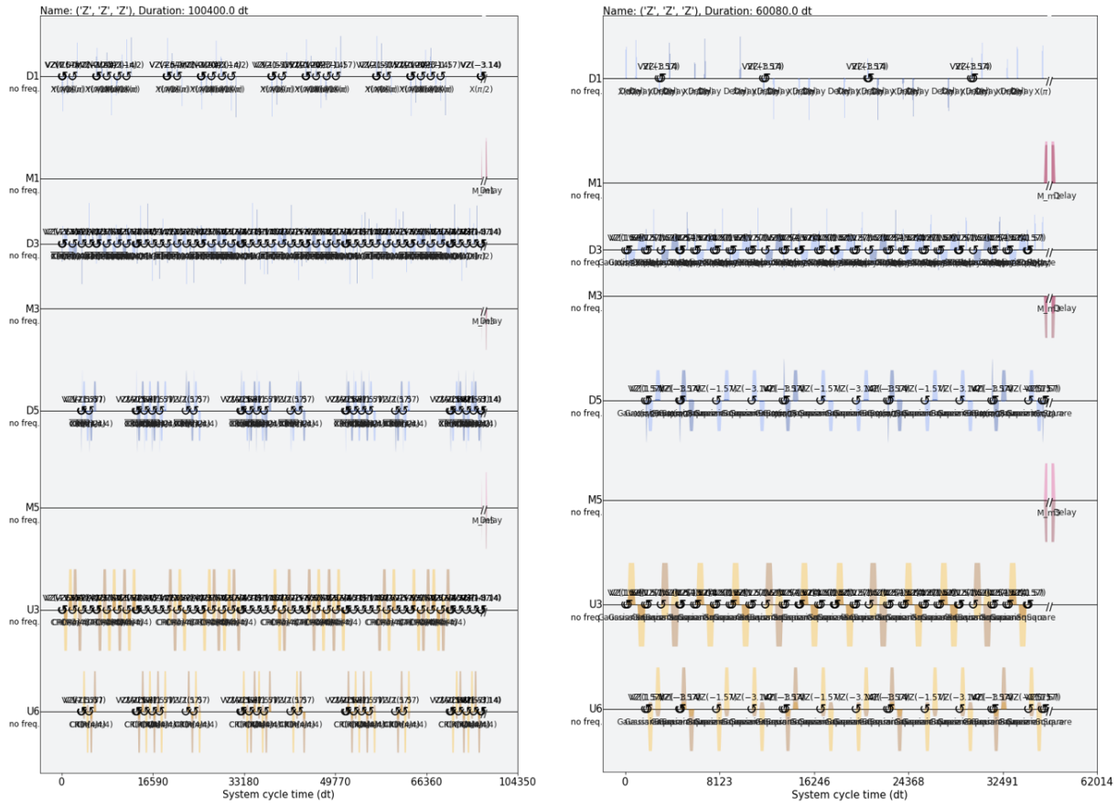

Figure 9: Comparison of the complete pulse schedule between using native CX gates and optimized RZX gates. The pulse schedule that uses native CX gates (left) takes about 100k dt in total and the one that uses RZX gates (right) takes about 60k dt.

References

[1] Minh C Tran et al. "Faster digital quantum simulation by symmetry protection". In: *PRX Quantum* 2.1 (2021), p. 010323.

[2] Pranav Gokhale et al. "Optimized quantum compilation for near-term algorithms with openpulse". In: *2020 53rd Annual IEEE/ACM International Symposium on Microarchitecture (MICRO)*. IEEE. 2020, pp. 186–200.

[3] Nathan Earnest, Caroline Tornow, and Daniel J Egger. "Pulse-efficient circuit transpilation for quantum applications on cross-resonance-based hardware". In: *Physical Review Research* 3.4 (2021), p. 043088.

[4] Sergey Bravyi et al. "Mitigating measurement errors in multiqubit experiments". In: *Physical Review A* 103.4 (2021), p. 042605.

[5] Abhinav Kandala et al. "Error mitigation extends the computational reach of a noisy quantum processor". In: *Nature* 567.7749 (2019), pp. 491–495.